논문 2010-47TC-11-8

광통신 대역에서의 유전체 직각 릿지 표면 플라즈몬 도파로 해석

(Analysis of Dielectric-Loaded Surface Plasmon Polariton Waveguides at Telecommunication Wavelengths)

정 재 훈*

(Jaehoon Jung)

요 약

유전체 직각 릿지 표면 플라즈몬 도파로의 주요 파라미터인 모드 유효굴절률과 도파길이를 해석하였다. 여러 금속 및 유전체를 릿지의 폭과 두께를 변화시키며 유한요소법을 이용하여 계산하였다. 상반되는 두 파라미터를 포함하는 메트릭으로 2차원 figure of merit을 사용하였다. 계산결과를 이용하면 광통신 파장대역에서 파장이하로 모여 낮은 전파손실을 가진 도파로의 여러 파라미터 및 크기를 설계할 수 있다.

Abstract

The main features of a dielectric-loaded surface plasmon polariton waveguide are analyzed such as mode effective index and propagation length. These parameters are calculated using the finite element method for different metal-polymer pairs while varying the ridge width and thickness. As a performance metric, we employ the 2D figure of merit including two conflicting parameters i.e. mode effective index and propagation length. The results obtained here allow one to identify the parameter range for realizing the dielectric-loaded surface plasmon polariton waveguide and to choose dimension and material of the ridge for subwavelength confinement and moderate propagation loss at telecom wavelengths.

Keywords : Surface Plasmon Polariton, Dielectric-Loaded Surface Plasmon Polariton Waveguide, Telecom Wavelength

Ⅰ. Introduction

Surface plasmon polaritons (SPPs) are electromagnetic excitations, coupled to free electrons in metals and propagating along a dielectric-metal interface[1]. The recent advances in nanophotonic fabrication methods have provided the possibility of writing various SPP-based waveguide configurations [2]. In the past years, a variety of plasmonic waveguides have heen proposed for compromise between mode confinement and propgation loss, which is known a fundamental tradeoff in plasmonics [3], such as stipe waveguides[4~5], and channel waveguides[6]. Among the proposed several waveguide configurations, the dielectric- loaded SPP waveguides (DLSPPWs) have been found to be attractive configurations in order to achieve subwavelength confinement keeping relatively low propagation loss at telecom wavelengths[7~10].

* 정회원, 단국대학교
(Dankook University)
접수일자: 2010년7월19일, 수정완료일: 2010년11월10일

In this paper, we investigate the fundamental properties of the DLSPPW such as mode effective index, confinement, and propagation lengths using the finite element method (FEM). We employ the figure of merit (FOM) of 2D SPP-based waveguide structures[11] to compare and assess the previous and our DLSPPWs. For different geometries and materials, the FOMs are calculated to obtain the optimal waveguide performance.

Ⅱ. Finite Element Analysis of DLSPPW Characteristics

A schematic diagram of a DLSPPW is shown in Fig. 1. The structure consists of a polymer ridge with thickness t and width w above the substrate and gold film of thickness d. In the calculation hereafter, the reference parameters are as follows: the refractive index of polymer, substrate, gold, and air are 1.535, 1.6[7] (we employ the same dielectric constants as those of Ref. 7 to compare the design results) 0.5590 + 9.8100i[12], 1, the metal thickness d =100 nm, and the excitation wavelength 1550 nm, respectively. The FEM using COMSOL has been used to analyze and optimize the DLSPPW structure.

Fig. 2 shows the electric field distribution (arrows) and power density (colored surface) for a DLSPPW with t=300 nm and w=300 nm. It is shown that the electric field has the dominant y component since the vertical variation in permittivity is larger than the lateral one in DLSPPW structures. We also observe

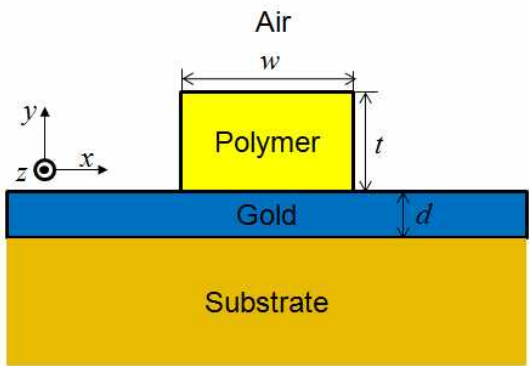

그림 1. DLSPPW의 구조
Fig. 1. Schematic of the DLSPPW structure.

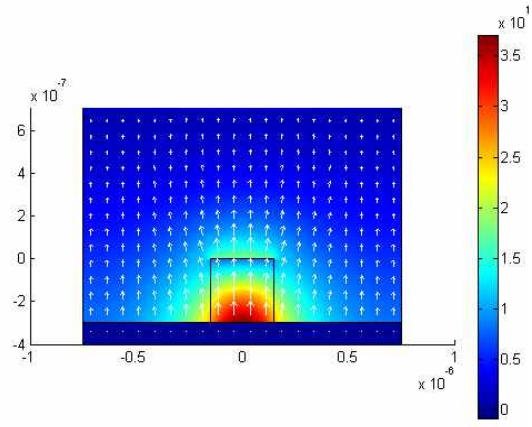

그림 2. t=300 nm, w=300nm 일때의 전계(화살표) 및 파워(면그래프) 분포
Fig. 2. The electric field distribution (arrows) and the power density (colored surface) of the fundamental mode of the DLSPPW with t=300 nm and w=300 nm.

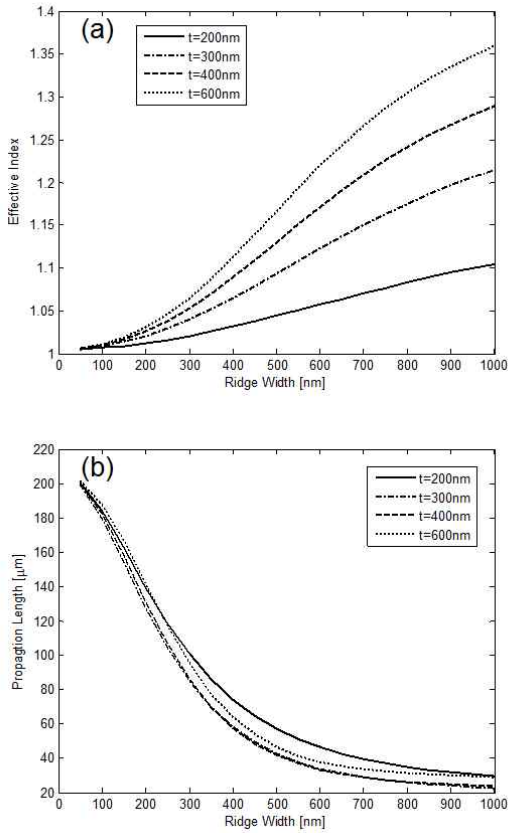

그림 3. DLSPPW의 여러 가지 두께에 대해 릿지의 폭에 의한 (a) 유효굴절률 및 (b) 전파상수
Fig. 3. (a) The mode effective index and (b) the propagation length of the fundamental mode of the DLSPPW as a function of the polymer ridge width w for different ridge thicknesses.

that the power density reaches the maximum at the center of the interface between the ridge and metal.

Fig. 3 indicates the variations of the effective indexes (a) and propagation length (b) defined as the same as those in previous works[1, 5~10] for the fundamental mode supported by the DLSPPW with different ridge thicknesses, respectively. We observe that as the width increases, the mode effective index increases and the propagation length decreases, which is consistent with the general consideration.

In Fig. 4 we show the mode effective index (a) and the propagation length (b) of the fundamental mode of the DLSPPW as a function of the polymer ridge thickness t for different ridge widths. One sees that the effective index has a monotonic increasing variation with the ridge thickness and the propagation length, however, has a minimum around t=200-300 nm. It seems due to the distinct 'squeezing' effect of the electric field in DLSPPW[7].

Ⅲ. Optimal Design of DLSPPW

In order to find the mode profile, the main electric field (Ey) is considered since in general, the y component of electric field is dominant in DLSPPWs. In Fig. 5 (a) we show The lateral distribution of the y-axis electric field along the middle of the ridge with t=300 nm, w=300 nm for different material pairs. We employ silica (n=1.5), GaAs (n=3.5) as a polymer and Au (0.5590 + 9.8100i), Al (1.4400 +16.0000i) at λ =1550 nm, respectively. The boundary condition

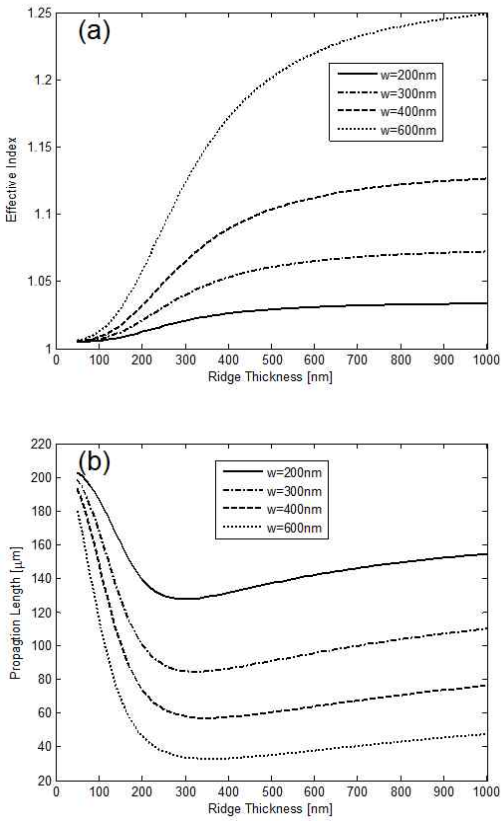

그림 4. DLSPPW의 여러 가지 폭에 대해 릿지의 두께에 의한 (a) 유효굴절률 및 (b) 전파상수

Fig. 4. (a) The mode effective index and (b) the propagation length of the fundamental mode of the DLSPPW as a function of the polymer ridge thickness t for different ridge widths.

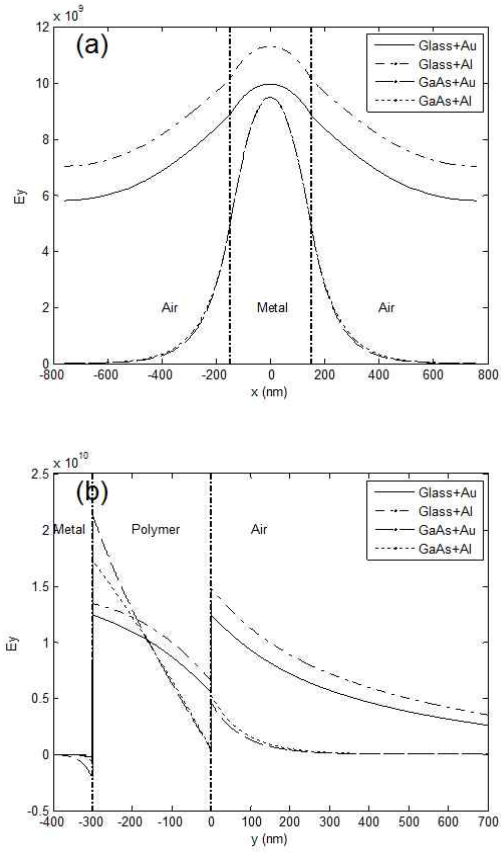

그림 5. t=300nm, w=300nm일 때의 (a) x축에 따른 (b) y축에 따른 Ey의 분포

Fig. 5. (a) The lateral distribution of the y-axis electric field along the middle of the ridge and (b) the vertical distribution of the y-axis electric field along the center of the ridge with t=300 nm, w=300 nm for different material pairs.

requires the conservation of the tangential components of the electric fields on both sides of the interface and this implies Ey is continuous since Ey is the tangential component in DLSPPW geometry.

In Fig. 5 (b) we show the vertical distribution of the y-axis electric field along the center of the ridge with t=300 nm, w=300 nm for different material pairs. Due to bounary condtion for the normal electric field components, discontinuities occurs at the polymer-etal interface and the air-polymer interface.

In Fig. 6, we show the mode effective index (a) and the propagation length (b) as a function of the polymer ridge width w with t=300 nm for different material pairs. The effective index increases as the refractive index of polymer is large and that of metal, however, is small in magnitude like the SPP mode in a single dielectric-metal interface. From Fig. 6 (b), we see that the metal material has more effect on propagation length than polymer material. It is also seen that the propagation length is large when the refractive index of polymer is small and that of metal is large.

In Fig. 7, we show the mode effective index (a) and the propagation length (b) as a function of the polymer ridge thickness t with w=300 nm for different material pairs.

In Fig. 8 (a) and (b), we show the FOM as a function of the ridge width and as a function of the ridge thickness for different material pairs, respectively. All other parameters are as in our reference structure. We observe that the FOM is not monotonic with the ridge width w but has a

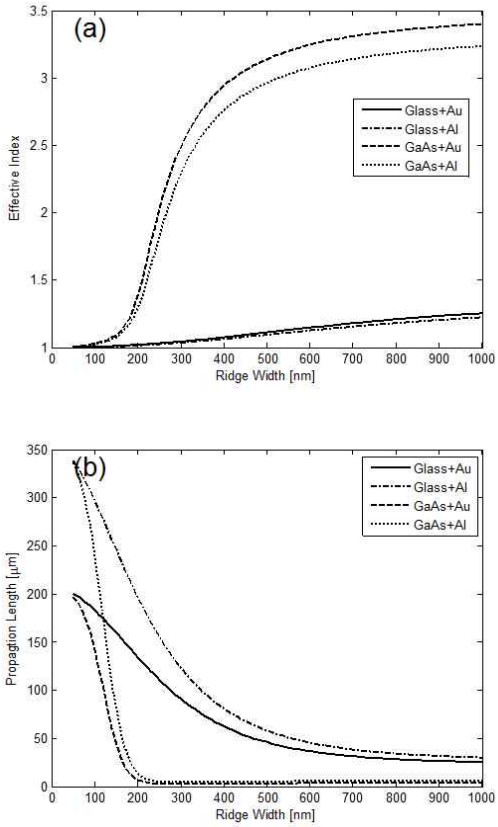

그림 6. t=300nm 일 때, 릿지의 폭에 따른 (a) 유효굴절률 및 (b) 전파상수

Fig. 6. (a) The mode effective index and (b) the propagation length as a function of the polymer ridge width w for different material pairs (t=300 nm).

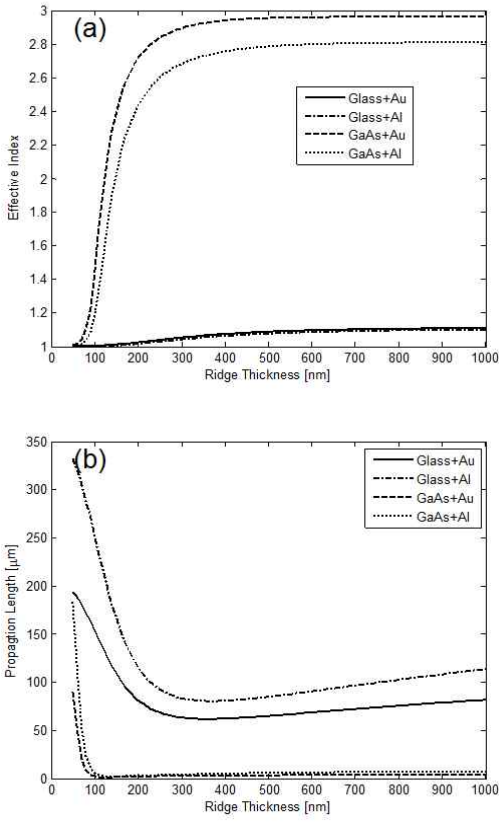

그림 7. w=300nm 일 때, 릿지의 폭에 따른 (a) 유효굴절률 및 (b) 전파상수

Fig. 7. (a) The mode effective index and (b) the propagation length as a function of the polymer ridge thickness t for different material pairs (w=300 nm).

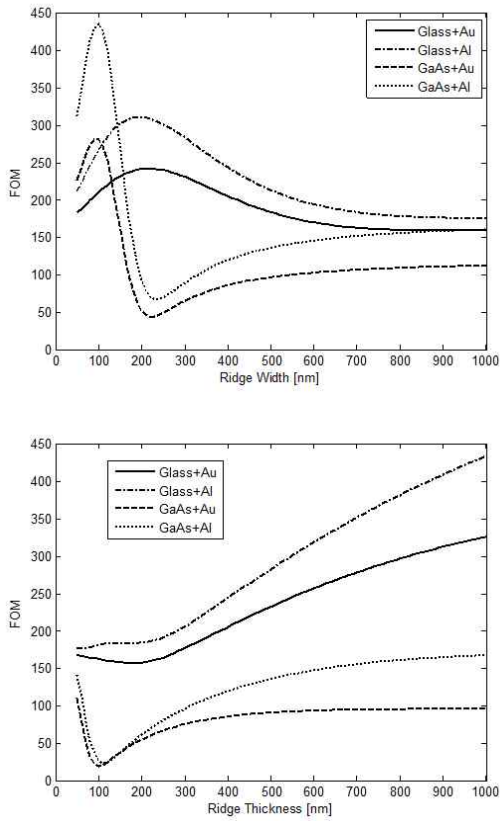

그림 8. (a) 릿지의 폭에 따른 FOM (b) 릿지의 두께에 따른 FOM

Fig. 8. (a) The FOM as a function of the ridge width and (b) as a function of the ridge thickness for different material pairs.

minimum around 100-200 nm. It is noteworthy to mention that as t increases, the FOM increases. When comparing the calculation resulst with the pervious ones[7] (glass+Au), the figures show that the FOM is improved from 242 to 435 due to high mode confinement and relatively low propagation loss. By introducing high refractive index polymer (GaAs) and metal (Al), the propagation mode can be confined in the lateral and transverse directions very well, and a longer propagation length can be achieved.

Ⅳ. Conclusions

The main characteristics of DLSPPWs have been investigated by making use of the FEM. The simulation results allow one to design the dimensions and material of the ridge as well as metal for high mode confinement and relatively low propagaton loss at the excitation wavelength of 1550 nm. The designed waveguide features the higher 2D FOM including mode confinement and propagation length than one previouly reported and, therefore can be used for optical components for high density photonic integration.

참 고 문 헌

[1] H. Raether, Surface Plasmons on Smooth and Rough Surfaces on Gratings, (Springer-Verlag, Berlin, 1988).

[2] T. W. Ebbesen, C. Genet, and S. I. Bozhevolnyi, “Surface-plasmon circuitry,” Phys. Today, Vol. 61, no. 5, pp.44-50, 2008.

[3] Odysseas Tsilipakos, Traianos V. Yioultsis, and Emmanouil E. Kriezisa, “Theoretical analysis of thermally tunable microring resonator filters made of dielectric-loaded plasmonic waveguides,” J. Appl. Phys., Vol. 106, pp. 093109, 2009.

[4] P. Berini, “Plasmon-polariton waves guided by thin lossy metal films of finite width: Bound modes of symmetric structures,” Phys. Rev. B Vol. 61, pp. 10484-10503, 2000.

[5] T. Nikolajsen, K. Leosson, and S. I. Bozhevolnyi, “Surface plasmon polariton based modulators and switches operating at telecom wavelengths,” Appl. Phys. Lett, Vol. 85, pp. 5833-5835, 2004.

[6] S. I. Bozhevolnyi, V. S. Volkov, E. Devaux, and T. W. Ebbesen, “Channel plasmon-polariton guiding by subwavelength metal grooves,” Phys. Rev. Lett, Vol. 95, pp. 046802, 2005.

[7] T. Holmgaard, and S. I. Bozhevolnyi, “Theoretical analysis of dielectric-loaded surface plasmon-polariton waveguides,” Phys. Rev. B Vol. 75, no. 24, pp. 245405, 2007.

[8] T. Holmgaard, Z. Chen, S. I. Bozhevolnyi, L. Markey, A. Dereux, A. V. Krasavin, and A. V. Zayats, “Wavelength selection by dielectric-loaded plasmonic components,” Appl. Phys. Lett., Vol. 94, no. 5, pp. 051111, 2009

[9] J. Grandidier, G. C. des Francs, S. Massenot, A. Bouhelier, L. Markey, J.-C. Weeber, C. Finot, and A. Dereux, “Gain-assisted propagation in a plasmonic waveguide at telecom wavelength,” Nano Lett. Vol. 9, no. 8, pp. 2935-2939, 2009.

[10] T. Holmgaard, S. I. Bozhevolnyi, L. Markey, A. Dereux, A. V. Krasavin, P. Bolger, and A. V.

Zayats, “Efficient excitation of dielectric-loaded surface plasmon-polariton waveguide modes at telecommunication wavelengths,” Phys. Rev. B Vol. 78, no. 16, pp. 165431, 2008.
[11] P. Berini, “Figures of merit for surface plasmon waveguides,” Opt. Express, Vol. 14, no. 26, pp. 13030-13042, 2006.
[12] E. D. Palik, *Handbook of Optical Constants of Solids* (Academic, New York, 1985).

저 자 소 개

정 재 훈(정회원)
1994년 서울대학교 전기공학과 학사 졸업.
1996년 서울대학교 전기공학부 석사 졸업.
2000년 서울대학교 전기공학부 박사 졸업.
2000년～2003년 삼성전자 정보통신총괄 책임연구원
2003년～2004년 단국대학교 전자전기공학부 전임강사
2005년～2008년 단국대학교 전자전기공학부 조교수
2009년～현재 단국대학교 전자전기공학부 부교수
<주관심분야 : 광통신, 광소자, Plasmonics>